

Paradoxes of magnetorotational instability and their geometrical resolution

Oleg N. Kirillov^{1,*} and Frank Stefani^{1,†}

¹*Helmholtz-Zentrum Dresden-Rossendorf
P.O. Box 510119, D-01314 Dresden, Germany*

(Dated: November 14, 2018)

The magnetorotational instability (MRI) triggers turbulence and enables outward transport of angular momentum in hydrodynamically stable accretion discs. By using the WKB approximation and methods of singular function theory, we resolve two different paradoxes of MRI that appear in the limits of infinite and vanishing magnetic Prandtl number. For the latter case we derive a new strict limit of the critical Rossby number. This new limit of $\text{Ro}_c = -0.802$, which appears for a finite Lundquist number of $\text{Lu} = 0.618$, extends the formerly known inductionless Liu limit of $\text{Ro}_c = -0.828$ valid at $\text{Lu} = 0$.

PACS numbers: 47.32.-y, 47.35.Tv, 47.85.L-, 97.10.Gz, 95.30.Qd

The magnetorotational instability (MRI) is the main candidate to explain the fast formation of stars and black holes by triggering turbulence and angular momentum transport in accretion disks. In its standard version (SMRI), with a vertical field being applied, the instability is non-oscillatory [1–3], while a helical applied magnetic field leads to an oscillatory instability (HMRI) [4].

Both in the astrophysical context [5], as well as in laboratory experiments [6], it is vital to know which laws of differential rotation are susceptible to MRI. The hydrodynamic reference point is Rayleigh’s criterion [7] stating that a rotating flow with an outwardly increasing angular momentum is stable. This implies, e.g., that a Taylor-Couette flow of an inviscid fluid between the inner and outer co-axial cylinders of radii $R_i < R_o$ and of infinite length that rotate with different angular velocities, $\Omega(R_i)$ and $\Omega(R_o)$, is stable, if and only if $R_i^2\Omega(R_i) < R_o^2\Omega(R_o)$. In contrast to this, assuming a perfectly conducting fluid and a vertical magnetic field B_z^0 being applied, Velikhov [1] and Chandrasekhar [2] found the more restrictive condition for stability in the form $\Omega(R_i) < \Omega(R_o)$. Remarkably, the latter criterion does not depend on the magnetic field strength, i.e. in the limit $B_z^0 \rightarrow 0$ it does not reduce to Rayleigh’s criterion valid for $B_z^0 = 0$. This ‘curious behavior of ostensibly changing the Rayleigh criterion discontinuously’ [8] constitutes the *Velikhov-Chandrasekhar paradox* which implies a dependence of the instability threshold on the sequence of taking the two limits of vanishing magnetic field and vanishing electrical resistivity. Its physical origin has been attributed to the fact that in a fluid of zero resistivity the magnetic field lines are permanently attached to the fluid, independent of the strength of the magnetic field [1, 2].

Another paradox of MRI emerges in the opposite limit of vanishing electrical conductivity. This *paradox of inductionless HMRI* [9] refers to the fact that in a helical magnetic field a perturbation can grow exponentially although the instantaneous growth of the energy of any perturbation must be smaller than in the field-free case.

Actually, the astrophysical relevance of HMRI is still

under debate. On the first glance, according to the criterion of Liu et al. [10], it could only work for rather steep rotation profiles $\Omega(R)$ with Rossby numbers $\text{Ro} := R(2\Omega)^{-1}d\Omega/dR < 2 - 2\sqrt{2} \simeq -0.828$. This would clearly exclude any relevance of HMRI for Keplerian profiles characterized by $\text{Ro} = -0.75$. It has to be noted, though, that the validity of the underlying local WKB approximation, and the possible role of electrical boundaries for extending the applicability of HMRI to higher Rossby numbers are controversially discussed [11]. Surprising new arguments arose recently from investigations of the saturation regime of MRI. For the case of small magnetic Prandtl numbers (as they are typical for protoplanetary disks), Umurhan speculated about a saturated rotation profile with regions of reduced shear, sandwiched by regions of strengthened shear [12]. For those latter regions with steeper than Keplerian profiles, HMRI could indeed become of relevance.

In this Letter we both find the ultimate upper limit of the critical Rossby number for HMRI, and resolve the mentioned paradoxes. We establish that these physical effects sharply correspond to the geometric singularities that are inherent on the stability boundaries of leading-order WKB equations.

We start with the local WKB equations for the axisymmetric perturbation of a steady-state rotational flow of a viscous and resistive fluid in the presence of an axial magnetic field that were derived and discussed by several authors [3, 13, 14]. They can be rewritten in the typical form of a non-conservative gyroscopic system [15],

$$\ddot{u} + (D + \Omega_0(1 + \alpha^2)J)\dot{u} + (N + K)u = 0, \quad (1)$$

where $u = (u_R, u_\phi)^T$ is the fluid velocity in polar coordinates (R, ϕ) . Separating the time-dependence according to $u = \tilde{u} \exp(\gamma t)$ yields the eigenvalue problem $L(\gamma)\tilde{u} = 0$ for the growth rate of the perturbation γ , where $L(\gamma) = \gamma^2 I + \gamma(D + \Omega_0(1 + \alpha^2)J) + N + K$, I the 2×2 unit matrix, $N = \Omega_0(\omega_\eta(1 + \alpha^2) + \text{Ro}(\omega_\eta - \omega_\nu))J$,

$$K = \begin{pmatrix} \omega_A^2 + \omega_\nu\omega_\eta & k_{12} \\ k_{12} & \omega_A^2 + \omega_\nu\omega_\eta + 4\alpha^2\Omega_0^2\text{Ro} \end{pmatrix} \quad (2)$$

with $k_{12} = \Omega_0(\omega_\eta(1 - \alpha^2) + \text{Ro}(\omega_\eta - \omega_\nu))$, and

$$J = \begin{pmatrix} 0 & -1 \\ 1 & 0 \end{pmatrix}, \quad D = \begin{pmatrix} \omega_\nu + \omega_\eta & \Omega_0(1 - \alpha^2) \\ \Omega_0(1 - \alpha^2) & \omega_\nu + \omega_\eta \end{pmatrix}. \quad (3)$$

In the above equations, $\omega_\nu = \nu k^2$ and $\omega_\eta = \eta k^2$ are the viscous and resistive frequencies, $\omega_A = k_z B_z^0 (\mu_0 \rho)^{-1/2}$ the Alfvén frequency, k_R and k_z the radial and axial wave numbers of the perturbation, $k^2 = k_z^2 + k_R^2$, $\alpha = k_z/k$, $\Omega_0 = \Omega(R_0)$ and $\text{Ro} = \text{Ro}(R_0)$, where R_0 is the radial coordinate of a fiducial point for the local stability analysis. We use the convention that $\rho = \text{const}$ is the density of the fluid, $\nu = \text{const}$ the kinematic viscosity, $\eta = (\mu_0 \sigma)^{-1}$ the magnetic diffusivity, σ the conductivity of the fluid, and μ_0 the magnetic permeability of free space. For $\alpha = 1$, $\omega_\nu = 0$, and $\omega_\eta = 0$, Eq. (1) is similar to the Hill equation for two orbiting mass points connected by a spring [16], a paradigmatic model of SMRI [5, 8].

Stable perturbations have $\Re \gamma \leq 0$ provided that γ with $\Re \gamma = 0$ is a semi-simple eigenvalue of $L(\gamma)$. The growing solutions of SMRI are non-oscillatory with $\Im \gamma = 0$. Therefore, $\gamma = 0$ implies that $\det(N + K) = 0$ at the threshold of SMRI [3] which results in the critical Rossby number (above which the flow is stable)

$$\begin{aligned} \text{Ro}_c &= -\frac{(\omega_A^2 + \omega_\nu \omega_\eta)^2 + 4\Omega_0^2 \omega_\eta^2 \alpha^2}{4\Omega_0^2 \alpha^2 (\omega_A^2 + \omega_\eta^2)} \\ &= -\frac{(\text{Pm}^{-1} + \text{Lu}^2 \text{Pm}^{-2})^2 + 4\text{Re}^2 \text{Pm}^{-2}}{4\text{Re}^2 (\text{Lu}^2 \text{Pm}^{-2} + \text{Pm}^{-2})}, \quad (4) \end{aligned}$$

where $\text{Re} = \alpha \Omega_0 \omega_\nu^{-1}$ is the Reynolds number, $\text{Pm} = \omega_\nu \omega_\eta^{-1}$ the magnetic Prandtl number, and $\text{Lu} = \omega_A \omega_\eta^{-1}$ the Lundquist number. Formula (4) coincides with that derived in [14] from the Routh-Hurwitz criterion [17].

The Velikhov-Chandrasekhar paradox occurs at infinite Pm and means that in the ideal MHD case ($\omega_\eta = 0$, $\omega_\nu = 0$) the limit $\omega_A \rightarrow 0$ yields Velikhov's value $\text{Ro}_c = 0$ as the instability threshold rather than Rayleigh's limit $\text{Ro}_c = -1$ of the non-magnetic case ($\omega_A = 0$, $\omega_\nu = 0$).

With $\omega_A = \varepsilon \cos \varphi$ and $\omega_\eta = \varepsilon \sin \varphi$ in (4), we obtain

$$\text{Ro}_c = -\frac{(\varepsilon \cos^2 \varphi + \omega_\nu \sin \varphi)^2 + 4\alpha^2 \Omega_0^2 \sin^2 \varphi}{4\alpha^2 \Omega_0^2}, \quad (5)$$

which for $\varepsilon \rightarrow 0$ reduces to

$$\text{Ro}_c = -\left(1 + \frac{1}{4\text{Re}^2}\right) \sin^2 \varphi = -\frac{1 + (2\text{Re})^{-2}}{1 + \text{Lu}^2}. \quad (6)$$

Introducing the new parameter $\text{Ro}' = (1 + 4\text{Re}^2)(1 + 4\text{Re}^2)^{-1}$ we find that in the $(\omega_A, \omega_\eta, \text{Ro}')$ -space Eq. (6) defines a so-called *ruled surface* $(\varepsilon, \varphi) \mapsto (\varepsilon \cos \varphi, \varepsilon \sin \varphi, \cos n\varphi)$ with $n = 2$, which is a canonical equation for the Plücker conoid of degree $n = 2$ [18]. The surface according to Eq. (4) tends to the Plücker conoid when $\varepsilon = \sqrt{\omega_A^2 + \omega_\eta^2}$ goes to zero. This surface is shown

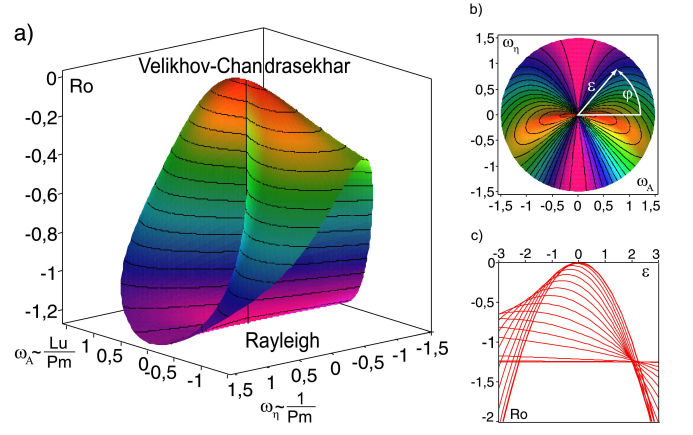


FIG. 1: (a) The critical Rossby number of SMRI as a function of $\omega_A \sim \text{LuPm}^{-1}$ and $\omega_\eta \sim \text{Pm}^{-1}$ for $\omega_\nu = 1$, $\alpha = 1$, $\Omega_0 = 1$, i.e. for $\text{Re} = 1$. (b) Top view of the surface. (c) Cross-sections of the surface along the rays specified by the Lundquist number, or, equivalently, by the angle φ that varies from 0 to 1.5 through the equal intervals $\Delta\varphi = 0.1$; the horizontal line corresponds to $\varphi = \pi/2$. Note that negative values of ω_η and ε are not physical.

in the $(\omega_A, \omega_\eta, \text{Ro})$ -space in Fig. 1(a) and in projection to the (ω_A, ω_η) -plane in Fig. 1(b) for $\text{Re} = 1$. For each α , ω_ν , and Ω_0 it has the same Plücker conoid singularity, i.e. an interval of self-intersection along the Ro -axis and two Whitney umbrella singular points at its ends. This singular structure implies non-uniqueness for the critical Rossby number when simultaneously $\omega_A = 0$ and $\omega_\eta = 0$. Indeed, for a given Lu , tending the magnetic field to zero along a ray $\omega_A = \omega_\eta \text{Lu}$ in the (ω_A, ω_η) -plane results in a value of the Rossby number specified by Eq. (6), see Fig. 1(c). The limit value of the critical Rossby number oscillates between the ideal MHD value $\text{Ro}_c = 0$ for $\text{Lu} = \infty$ ($\varphi = 0$) and the non-magnetic value $\text{Ro}_c = -1 - (2\text{Re})^{-2}$ for $\text{Lu} = 0$ ($\varphi = \pi/2$), which explains the Velikhov-Chandrasekhar paradox.

Now we turn over to the paradox of inductionless HMRI which is related to a similar geometric singularity as discussed above. The leading order WKB equations that describe the onset of instability of a hydrodynamically stable TC-flow with a helical external magnetic field are $\dot{\xi} = H\xi$ with $\xi^T = (u_R, u_\phi, B_R(\mu_0 \rho)^{-1/2}, B_\phi(\mu_0 \rho)^{-1/2})$ and

$$H = \begin{pmatrix} -\omega_\nu & 2\Omega_0 \alpha^2 & i\omega_A & -2\omega_{A\phi} \alpha^2 \\ -2\Omega_0(1 + \text{Ro}) & -\omega_\nu & 0 & i\omega_A \\ i\omega_A & 0 & -\omega_\eta & 0 \\ 2\omega_{A\phi} & i\omega_A & 2\Omega_0 \text{Ro} & -\omega_\eta \end{pmatrix}, \quad (7)$$

where the additional parameter $\omega_{A\phi} = R_0^{-1} B_\phi^0 (\mu_0 \rho)^{-1/2}$ is the Alfvén frequency of the azimuthal magnetic field component [14]. For $\omega_{A\phi} = 0$ these equations yield (1).

The dispersion equation $\det(H - \gamma I) = 0$ reads

$$\lambda^4 + a_1 \lambda^3 + a_2 \lambda^2 + (a_3 + ib_3) \lambda + a_4 + ib_4 = 0, \quad (8)$$

where I is a 4×4 unit matrix, $\lambda = \gamma(\omega_\nu \omega_\eta)^{-1/2}$, and

$$\begin{aligned} a_1 &= 2(1 + \text{Pm}^{-1})\sqrt{\text{Pm}}, \\ a_2 &= 2(1 + (1 + 2\beta^2)\text{Ha}^2) + 4\text{Re}^2(1 + \text{Ro})\text{Pm} + a_1^2/4, \\ a_3 &= a_1(1 + (1 + 2\beta^2)\text{Ha}^2) + 8\text{Re}^2(1 + \text{Ro})\sqrt{\text{Pm}}, \\ a_4 &= (1 + \text{Ha}^2)^2 + 4\beta^2\text{Ha}^2 + 4\text{Re}^2(1 + \text{Ro}(\text{Pm}\text{Ha}^2 + 1)), \\ b_3 &= -8\beta\text{Ha}^2\text{Re}\sqrt{\text{Pm}}, \quad b_4 = b_3(1 + (1 - \text{Pm})\text{Ro}/2)/\sqrt{\text{Pm}}, \end{aligned} \quad (9)$$

where we have introduced now the Hartmann number $\text{Ha} = \text{Lu}\text{Pm}^{-1/2}$ and the helicity parameter $\beta = \alpha\omega_{A_\phi}\omega_A^{-1}$ of the external magnetic field. According to the analogue of the Routh-Hurwitz conditions for the complex polynomials—the Bilharz criterion [17]—the threshold of HMRI is defined by $m_4(\beta, \text{Re}, \text{Ha}, \text{Pm}, \text{Ro}) = 0$, where m_4 is the determinant of the so-called Bilharz matrix [14, 17, 19] composed of the coefficients (9). The stability condition $\Re\lambda < 0$ holds if and only if $m_4 > 0$ [14, 17, 19]. For $\beta = 0$ the dispersion equation and thus the threshold for HMRI reduce to that of SMRI [14].

In the following we will see that in the limit $\text{Pm} \rightarrow 0$ it is again Lu that governs the value of Ro_c . For this purpose, we show in Fig. 2(a) a typical critical surface $m_4 = 0$ in the $(\text{Pm}, \text{Re}^{-1}, \text{Ro})$ -space for the special parameter choice $\text{Ha} = 15$ and $\beta = 0.7$. On the Ro -axis we find a self-intersection and two Whitney umbrella singularities at its ends. At the upper singular point, i.e. exactly at $\text{Pm} = 0$, we get (see [14])

$$\begin{aligned} \text{Ro}_c(\beta, \text{Ha}) &= \frac{(1 + \text{Ha}^2)^2 + 4\beta^2\text{Ha}^2(1 + \beta^2\text{Ha}^2)}{2\beta^2\text{Ha}^4} \\ &- \frac{((2\beta^2 + 1)\text{Ha}^2 + 1)\sqrt{(1 + \text{Ha}^2)^2 + 4\beta^2\text{Ha}^2(1 + \beta^2\text{Ha}^2)}}{2\text{Ha}^4\beta^2}. \end{aligned} \quad (10)$$

In the limit $\text{Ha} \rightarrow \infty$, this critical value is majorated by

$$\text{Ro}_c(\beta) = \frac{1 + 4\beta^4 - (1 + 2\beta^2)\sqrt{1 + 4\beta^4}}{2\beta^2}, \quad (11)$$

with the maximum at the well-known Liu limit $\text{Ro}_c = 2 - 2\sqrt{2} \simeq -0.828$ when $\beta = \sqrt{2}/2 \simeq 0.707$ [10, 14].

In Fig. 2(a) we see that the case with $\text{Pm} = 0$ is connected to the case $\text{Pm} \neq 0$ by the Plücker conoid singularity, quite similar as it was discussed for the paradox of Velikhov and Chandrasekhar. Interestingly, Ro_c for the onset of HMRI can increase when Pm departs from zero which happens along curved pockets of HMRI, see Fig. 2(a). The two side bumps of the curve $\text{Re}^{-1}(\text{Pm})$ in a horizontal slice of the surface correspond to the domains of the *essential HMRI* while the central hill marks the *helically modified SMRI* domain, according to the classification introduced in [14]. For small Pm the essential HMRI occurs at higher Ro than the helically modified SMRI, while for some finite value of Pm the central hill and the side bumps get the same value of Ro_c . Most remarkably,

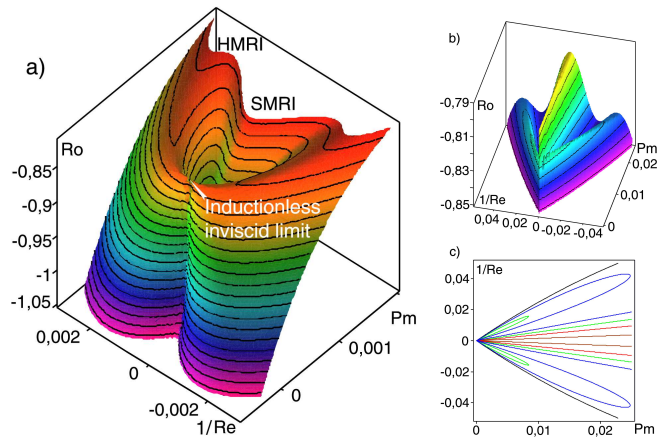


FIG. 2: (a) The critical Rossby number of the essential HMRI and helically modified SMRI for $\text{Ha} = 15$ and $\beta = 0.7$ (left) in the $(\text{Pm}, \text{Re}^{-1}, \text{Ro})$ -space. (b) The critical Rossby number for $\text{Lu} = 0.5$ and $\beta = 0.6$ in the $(\text{Pm}, \text{Re}^{-1}, \text{Ro})$ -space and (c) its cross-sections in the $(\text{Pm}, \text{Re}^{-1})$ -plane for (black) $\text{Ro} = -0.842$, (blue) $\text{Ro} = -0.832$, (green) $\text{Ro} = -0.822$, (red) $\text{Ro} = -0.812$, (brown) $\text{Ro} = -0.802$.

there is a value of Ro_c at which the two side bumps of the curve $\text{Re}^{-1}(\text{Pm})$ disappear completely. This is the maximal possible value for the essential HMRI, at least at the given β and Ha . Now we can ask: how does this limit behave if we send Ha to infinity, and to which value of Lu does this correspond?

Actually, with the increase in Ha the stability boundary preserves its shape and simultaneously it compresses in the direction of zero Pm . Substituting $\text{Ha} = \text{Lu}\text{Pm}^{-1/2}$ into the equations (9), we plot again the surface $m_4 = 0$ in the $(\text{Pm}, \text{Re}^{-1}, \text{Ro})$ -space, but now for a given β and Lu , Fig. 2(b).

The corresponding cross-sections of the instability domain in the $(\text{Re}^{-1}, \text{Pm})$ -plane are shown in Fig. 2(c). At a given value of Ro there exist three domains of instability with the boundaries shown in blue and green. Two sub-domains that have a form of a petal correspond to the HMRI. They are bounded by closed curves with a self-intersection singularity at the origin. They are also elongated in a preferred direction that in the $(\text{Re}^{-1}, \text{Pm})$ -plane corresponds to a limited range of the magnetic Reynolds number $\text{Rm} = \text{Pm}\text{Re}$. The central domain, which corresponds to the helically modified SMRI, has a similar singularity at the origin and is unbounded in the positive Pm -direction. In comparison with the central domain, the side petals have lower values of Rm .

Now we reconsider again the limit $\text{Pm} \rightarrow 0$, while keeping Lu as a free parameter. At the origin all the boundaries of the petals can be approximated by the straight lines $\text{Pm} = \text{Rm}\text{Re}^{-1}$. Substituting this expression into equation $m_4 = 0$, we find that the only term that does not depend on Pm is a polynomial

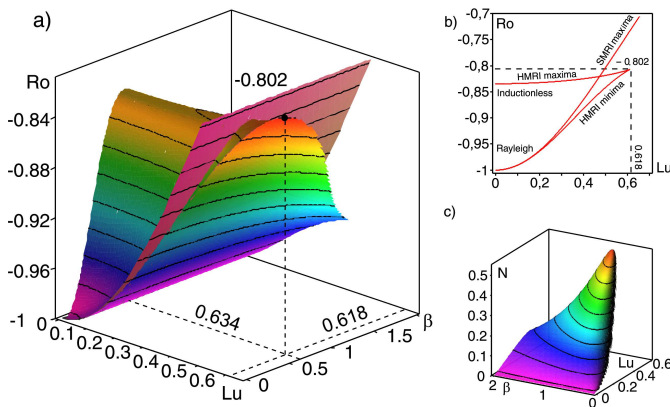


FIG. 3: (a) Discriminant surface in the (Lu, β, Ro) -space and (b) its cross-section at $\beta = 0.634$. (c) Interaction parameter $N = Lu^2 Rm^{-1}$ at the essential HMRI maxima.

$Q(Rm, Lu, \beta, Ro) = p_0 + p_1 Rm^2 + p_2 Rm^4 + p_3 Rm^6$, where, e.g., $p_0 = Lu^4(4\beta^4 Lu^2 + 2\beta^2 + 4Lu^2\beta^2 + 1)^2$ [19].

The roots of the polynomial are coefficients Rm of the linear approximation to the instability domains at the origin in the (Re^{-1}, Pm) -plane. Simple roots mean non-degenerate self-intersection of the stability boundary at the origin. Double roots correspond to a degeneration of the angle of the self-intersection when it collapses to zero which happens only at the maximal critical Rossby number, Fig. 2(b). In the (Lu, β, Ro) -space a set of points that correspond to multiple roots of the polynomial Q is given by the discriminant surface $64\Delta^2 p_0 p_3 = 0$ [19]. The surface $p_3 = 0$ consists of a sheet $Ro = -(1 + Lu^2)^{-1}$ corresponding to the doubly degenerate infinite values of Rm at the maxima of the helically modified SMRI. It smoothly touches along the β -axis the surface $\Delta = 0$ that consists of two smooth sheets that touch each other along a spatial curve — the cuspidal edge — corresponding to triple roots of the polynomial Q , Fig. 3(a).

Every point on the upper sheet of the surface $\Delta = 0$ represents a degenerate linear approximation to the essential HMRI domain and therefore a maximal Ro at the corresponding values of β and Lu . Numerical optimization results in the new ultimate limit for HMRI $Ro_c \simeq -0.802$ at $Lu \simeq 0.618$, $\beta \simeq 0.634$, and $Rm \simeq 0.770$, see Fig. 3(b). This new limit of Ro_c on the cuspidal edge is smoothly connected to the inductionless Liu limit by the upper sheet of the discriminant surface, which converges to the curve (11) when $Lu = 0$. We point out that the new limit is achieved at $Ha \rightarrow \infty$ when the optimal Pm tends to zero in such a way that $Lu \simeq 0.618$. Figure 3(c) shows the behaviour of the so-called interaction parameter (or Elsasser number) $N = Lu^2/Rm$ for the HMRI sheet. It is remarkable that, at $Lu = 0$, HMRI starts to work already at $N = 0$. This can be explained by the observation that the optimal value for HMRI corresponds to $NHa = Lu^3/(Rm\sqrt{Pm}) = 1/(1 + 2^{-1/2}) = 0.586$, [14].

Later, for increasing Lu , the optimal N acquires final values, passes through its maximum and at $Lu \simeq 0.618$ and $\beta \simeq 0.634$ it terminates at $N = 0.496$.

Inspired by the theory of dissipation induced instabilities [15], we have resolved the two paradoxes of SMRI and HMRI in the limits of infinite and zero magnetic Prandtl number, respectively, by establishing their sharp correspondence to singularities on the instability thresholds. In either case, it is the local Plücker conoid structure that explains the non-uniqueness of the critical Rossby number, and its crucial dependence on the Lundquist number. For HMRI, we have found an extension of the former Liu limit $Ro_c \simeq -0.828$ (valid for $Lu = 0$) to a somewhat higher value $Ro \simeq -0.802$ at $Lu = 0.618$ which is, however, still below the Kepler value. To study the possible consequences of this new limit for the saturation of MRI in accretion disks or experiments, is left for future work.

Financial support from the Alexander von Humboldt Foundation and the DFG in frame of STE 991/1-1 and of SFB 609 is gratefully acknowledged.

* Electronic address: o.kirillov@hzdr.de

† Electronic address: f.stefani@hzdr.de

- [1] E.P. Velikhov, Sov. Phys. JETP-USSR **9**(5), 995 (1959).
- [2] S. Chandrasekhar, PNAS **46**, 253 (1960).
- [3] S.A. Balbus, J.F. Hawley, Astrophys. J. **376**, 214 (1991).
- [4] E. Knobloch, Astrophys. J. **376**, 214 (1991); R. Hollerbach, G. Rüdiger, Phys. Rev. Lett. **95**, 124501 (2005).
- [5] S.A. Balbus, J.F. Hawley, Rev. Mod. Phys. **70**, 1 (1998).
- [6] D.R. Sisan et al., Phys. Rev. Lett. **93**, 114502 (2004); F. Stefani et al., Phys. Rev. Lett. **97**, 184502, (2006); F. Stefani et al., Phys. Rev. E. **80**, 066303, (2009); M. D. Nornberg, H. Ji, E. Schartman, A. Roach, J. Goodman, Phys. Rev. Lett. **104**(7), 074501, (2010).
- [7] J.W.S. Rayleigh, Proc. R. Soc. Lond. A. **93**, 148 (1917).
- [8] S.A. Balbus, Ann. Rev. Astron. Astroph., **41**, 555 (2003).
- [9] J. Priede, I. Grants, G. Gerbeth, Phys. Rev. E **75**, 047303 (2007); J. Priede, I. Grants, G. Gerbeth, J. Phys.: Conf. Ser. **64**, 012011 (2007).
- [10] W. Liu, J. Goodman, I. Herron, H. Ji, Phys. Rev. E **74**, 056302 (2006).
- [11] G. Rüdiger and R. Hollerbach, Phys. Rev. E **76**, 068301 (2007).
- [12] O.M. Umurhan, Astron. Astrophys. **513**, A47 (2010).
- [13] H. Ji, J. Goodman, A. Kageyama, MNRAS **325**, L1 (2001); V. Urpin and G. Rüdiger, Astron. Astrophys. **437**, 23 (2005); V.P. Lakhin, E.P. Velikhov, Phys. Lett. A **369**, 98 (2007); G. Rüdiger, M. Schultz, Astron. Nachr. **329**, 659 (2008).
- [14] O.N. Kirillov, F. Stefani, Astrophys. J. **712**, 52 (2010).
- [15] R. Krechetnikov, J.E. Marsden, Rev. Mod. Phys. **79**, 519 (2007); O.N. Kirillov, F. Verhulst, Z. Angew. Math. Mech. **90**, 462 (2010).
- [16] G.W. Hill, Am. J. Math. **1**, 5 (1878); V.V. Sidorenko, A. Celletti, Cel. Mech. Dyn. Astron. **107**, 209 (2010).
- [17] H. Bilharz, Z. Angew. Math. Mech. **24**, 77 (1944).
- [18] I. Hoveijn, O.N. Kirillov, J. Diff. Eqns. **248**, 2585, (2010).
- [19] Supplemental material.